SLIP RATE AND EARTHQUAKE RECURRENCE OF THE DÜZCE FAULT (NORTH ANATOLIAN FAULT ZONE): INTEGRATING GEOMORPHOLOGICAL AND PALEOSEISMOLOGICAL ANALYSES

Pucci, S. [a, *], **D. Pantosti** [a], **P.M. De Martini** [a]

[a] Istituto Nazionale di Geofisica e Vulcanologia, Via di Vigna Murata 605, 00143 Rome, Italy

* Corresponding author. Current address: *Istituto Nazionale di Geofisica e Vulcanologia, Via di Vigna Murata 605, 00143 Rome, Italy* , Tel.: +39-6-51860406, Fax: +39-6-51860507.

E-mail address: pucci@ingv.it (S. Pucci).

Abstract

To learn about recurrence of large earthquakes and strain model on the Düzce segment of the North Anatolian Fault Zone, that ruptured on November, 12, 1999 (Mw 7.1), systematic geomorphological and paleoseismological analyses were integrated.

In order to provide new estimates on Quaternary slip rate of the fault., geo-morphological mapping along the fault trace permitted to analyze fault-related cumulative landforms and drainage pattern settings. Remnant of an old alluvial fan modeled by fluvial terraces and 41 right-hand stream deflections were reconstructed, described and used as offset geomorphic markers. Two correlated Late Pleistocene, terrace risers, offset of about 300 and 900 m, respectively, were dated by means of OSL method about 21 kyr BP and 60 kyr BP. Moreover, the onset of the offset of the streams deflected for a total of ~100 m was radiocarbon dated about 7000 yr BP. These data translate to a constant rate of deformation of 15.0±3.2 mm/yr for the last 60 kyr. On the basis of "characteristic-earthquake model" and under constant slip rate assumptions, it is possible to estimate that stream deflections across the Düzce Fault may be explained by repetition of 20-30 1999-like earthquakes during the last 7000 years, thus the recurrence time for surface rupturing events of the Düzce Fault is 290±60 years.

With the aim to reconstruct the record of last large earthquakes, 10 trenches at five sites were excavated. By merging information obtained from all trenches, evidence for three surface faulting earthquakes prior to 1999 were found. These paleoearthquakes are dated on the basis of radiocarbon, 210Pb and archaeological information and can be summarized at: 1) AD1685-1900, possibly end of 19th century; 2) AD1685-1900, possibly

close to AD1700; 3) AD800-1000. Some of them can be correlated to historical earthquakes occurred on AD967, 1719, 1878 or 1894. These paleoseismological results, merged with those from previous papers, are suggestive of bimodal recurrence distribution yielding overall average recurrence time of ~350 yrs for the past two millennia, compatible with that calculated from the geomorphic markers analysis. Under the assumption of "characteristic earthquake", bimodal paleoearthquakes distribution indicate slip rate fluctuations during the past two millennia, with clustered high strain release. These results suggest Wallace-type strain release model for the Düzce fault, and average strain accumulation of 11.4±1.2 mm/yr, in agreement with slip rate results for the past 60 kyr obtained by geomorphic marker analysis.

1. Introduction

Slip rates of active faults and earthquake recurrence are generally estimated through trenching investigations and analysis of offset geomorphic markers.

Both approaches have limitations. Although very powerful, investigation by paleoseismologic trenching contains a fundamental limit that strongly affects estimates of slip-rates, recurrence intervals and behavioural models of strain release. Such limit is the usual small number of paleoearthquakes that can be recognized, such to cover an insufficient length of time to be statistically trustworthy. However, it is possible to reduce uncertainties spreading the analyses to the entire fault extent and providing accurate paleoearthquake dating. Despite that, while trench investigations provide age of paleoearthquakes and possibly slip per event of dislocation cumulated during several events, generally cannot extend observations longer than short-term periods (<10,000 years). Conversely, offset geomorphic markers allow measurements of long time-scales strain accumulation, with no information on the timing and patterns of faulting events. Studies of such markers provide averaged information on the slip rate or the cumulative slip during repeated events, spanning analysis over middle and long-term periods (>100,000 years). For this reason it is critical to overcome such limitations through the integration and comparison of these independent approaches.

For this purpose, to learn about slip rates and recurrence of large earthquakes on the Düzce segment of the North Anatolian Fault Zone, that ruptured on November, 12, 1999 (Mw 7.1) systematic geomorphological and paleoseismological analyses were integrated. This is based on the fact that earthquakes are an integral component of the landscape evolution, this is true all along the North Anatolian Fault Zone (NAFZ) and it is very clear for the Düzce Fault. In fact, the outstanding morphology of this active strike-slip fault is one of the direct consequences of: 1) long-lasting significant deformation; 2) important present-day strain-rate; and 3) frequent seismicity that ordinarily accommodate the present-day strain rate; 4) recurrent surface faulting potentially recorded by the deformation of recent deposits.

The area of the Düzce segment was favourable for slip rate studies because of (1) extensively faulted Pleistocene and Holocene continental deposits, (2) high preservation potential of the landforms with respect to the time-scale of the tectonic process, and (3) near-fault deformation recorded and expressed by the landscape as recognized following the 1999 earthquake [Pucci et al., 2006; Pucci, 2007], that offer useful records of long-term slip-rates.

In the following, after a brief introduction on the tectonic framework of the NAFZ and on the Düzce Fault segment, we present the analysis of the preliminary Düzce Fault slip rate and recurrence intervals estimates obtained through geomorphological and paleoseismological studies. In fact, the recognition of lateral displacements of streams and alluvial terraces, resulting from the strike-slip faulting activity during the past 60ky [Pucci et al., 2008] and the reconstruction of the record of past large earthquakes, by means of 10 trenches excavated along the entire fault length [Pantosti et al., 2008], allow such integrated study of independent dataset.

2. Geological setting

The NAFZ is an active right-lateral system, about 1500 km long, which bounds the westward-extruding Anatolian block to the north [McKenzie, 1972; Şengör, 1979; Barka, 1992; Şaroğlu et al., 1992] (Fig. 1a) that, based on the age of fault-related basin deposits, is considered to have been active since the Late Miocene [Şengör et al., 1985; Dewey et al., 1986; Şengör et al., 2005] or Early Pliocene [Barka, 1992]. Seismicity along the NAFZ is characterized by frequent moderate to large earthquakes (M 7) with focal mechanism solutions that show essentially pure right-lateral strike-slip motion [Canıtez and Uçer, 1967; McKenzie, 1972; Reinecker et al., 2004].

The trace of the NAFZ splays progressively to the west up to three major strands in the Marmara Sea (NNAF, CNAF, and SNAF in Fig. 1) [Wong et al., 1995; Armijo et al., 1999; Okay et al., 1999]. However regional GPS networks indicate the northern strand to accommodate most of the 20–30 mm/yr strike-slip strain [Straub et al., 1997; Reilinger et al., 1997, 2000; Kahle et al., 1999, 2000; McClusky et al., 2000]. Similar deformation rates of 20±10 mm/yr [Jackson and McKenzie, 1988; Westaway, 1994; Parson et al., 2000] are suggested by seismic moment release over the past 100–400 yrs.

Differently, the slip rates documented from geology and geomorphology along the NAFZ are much smaller than the present-day geodetic measurements, showing a large uncertainties and variability (from 2 mm/yr up to 24 mm/yr). This difference suggests an acceleration of the deformation over time or an underestimation in measuring and dating geological offsets, as testified by a limited spatial and age distribution of the studied geologic and geomorphologic markers [see Pucci et al., 2008].

During the 20th century, a progression of large earthquakes migrating westward occurred along the NAFZ, that culminated on the destructive 1999 Izmit seismic sequences (Fig. 1). The second mainshock of this sequence, the Mw 7.1 on 12 November 1999, ruptured the Düzce fault segment. This earthquake is considered to have been triggered by the Mw 7.4 Izmit earthquake that occurred 3 months earlier (17 August) on the next fault segment to the west. The Düzce earthquake produced a ~40-km-long surface rupture with up to 5 m of right-lateral offset and up to 2.5 m of vertical throw [Akyüz et al., 2000, 2002; Pucci et al., 2007]. The horizontal coseismic slip distribution curve (Fig. 2b), built by integrating the data collected after the 1999 earthquake, exhibits a large along–strike variability, with 5.0 m maximum and 2.4 m dextral offsets averaged on the entire fault length. The main characteristics of the slip distribution, expressed by the interpolation of the maximum values that better describes the seismic moment at the surface (for details see Pucci et al., 2007), are: 1) a bow-shape, with slip tapering off at both ends (west of Efteni Lake and east of Kaynasli); 2) the central part, with a constant mean value of about 4.0 m.

The Düzce fault is located just west of the Bolu basin, where the NAFZ starts splaying into two main strands, the Düzce/Karadere to the north and the Mudurnu to the south, that equally take up the present-day deformation [Ayhan et al., 1999, 2001; Pucci et al., 2008]. The Düzce fault has an average E-W trend and a clear geomorphic expression, being the edge between the Quaternary Düzce and Kaynasli basins to the north and the Paleozoic-Eocene rocks of the Almacik block to the south (Fig. 2a). The western and eastern boundaries of the 1999 Düzce earthquake rupture coincide to the releasing fault junctions [*sensu* Christie-Blick and Biddle, 1985] and complex step-overs, respectively, that they form with the northern strand of the NAFZ.

Although Turkey has one of the richer records of historical seismicity in the Mediterranean, no clear evidence for historical earthquakes produced by the Düzce segment of the NAFZ during the past centuries has been found. The only historical earthquakes that are known to be close enough to be potentially associated to the Düzce fault are A.D. 967, A.D. 1719, A.D. 1754, A.D. 1878, A.D. 1894 [Ambraseys and Finkel, 1995; Ambraseys, 2002, 2006] (Fig. 1).

3. Geomorphological data

3.1. The Düzce fault landforms

We carried out geomorphic analysis along the 1999 rupture zone (hereinafter referred as near-fault analysis). Particular attention has been devoted to the drainage pattern analysis and to the setting of depositional and tectonic landforms, as well as to the recognition of recent continental deposits, crucial to detect suitable sediments for dating. The 1:25,000-scale geological and geomorphological map of the Düzce Fault (fig. 3) shows landforms, related to the erosional and the depositional processes that have been shaping the Almacik range-front, strongly coupled with near-fault tectonic landforms related to fault location and activity.

The erosion of the Almacik block provided important sediment production for the Düzce Basin. These sediments that cover the foot of the range-front are mainly alluvial fans that merge into coalescent aprons (hereinafter referred as bajadas) composed of Middle-Late Pleistocene alluvial fan and Late Pliocene-Early Pleistocene conglomerate-sandstone units (zones x, fig. 3) [Herece and Akay, 2003], and also of active Holocene fans, deposited in subsequent incisions of the old bajadas (e.g. spot y, fig. 3). These generally loose and soft recent deposits recorded persistent landform modification due to faulting and developed well-expressed tectonic-related morphologies whose topography controlled the drainage pattern. Such features are clearly not related to the dynamics of the bajada, since they present tectonic deformations of the original depositional layers. The most common tectonic landforms in the study area are: tilted surfaces, fault escarpments, benches, saddles alignments, linear valleys, shutter ridges, pressure ridges, and sag ponds. This tectonic landforms appear to be the surface expression of a localized slip plane at depth, and the width of the near-fault deformation zones at the surface is related both to the thickness of young alluvial cover sequences and to free surface effects, as observed along other seismogenic structures (e.g. Landers [Sieh et al., 1993; Jhonson et al., 1994; Lazarte et al., 1994]; Dast-e Bayaz [Tchalenko and Ambraseys, 1970; Tchalenko and Barberian 1975]). Such tectonic landforms reflect also a small vertical component of deformation, resulting from strike-slip movement along a non rectilinear fault plane that produces transtension at releasing bends (e.g. spots z, fig. 3a) and transpression at restraining bends (e.g. spots q, fig. 3).

Along the western section of the Düzce fault, the 1999 coseismic fault trace bounds the triangular embayments of the range front, that host bajadas. Here, the rupture follows a saw-tooth trajectory (e.g. spots k, fig. 3a) with a few E-W trending elements (e.g. spots w in fig. 3a), associated to subtle and youthful landforms. This suggests that the E-W trending elements adjusted only a small cumulative deformation and may represent an incipient stage of evolution of the fault system from irregular to linear geometry [Pucci et al., 2006 and 2007]. Because the bajada of this section is bounded by the fault to the north, it has a topographic profile with steep fanheads and is characterized by linear and abrupt transitions to the alluvial-lacustrine deposits of the Düzce plain. Linear escarpments, with strong stream incisions across the bajada and suspended terraces can be found at the stream outlets along the range-front foot (spots h, fig. 3a), implying the occurrence of an important subsidence north of the Düzce Fault.

Conversely, the eastern section of the Düzce Fault (fig. 3b) presents a more regular, localized, prominent E-W trace paralleling the mean trend of the whole Düzce fault. This E-W trending section crosscuts both recent continental deposits and bedrock and is associated with well developed landforms indicating its persistent long-term activity. It is characterized by shutter and pressure ridges, 300 to 1000 m-long, up to 120 m high (e.g. spots r, fig. 3b), with elongated shapes and long axes paralleling the escarpment elements they are associated with. In many cases, the ridges act as natural dams for northward flowing drainages, being thus responsible for the localization of ponds and the trapping of Holocene fans against the scarp (e.g. spots t, fig. 3b). The tectonic influence on drainage pattern along the fault is also expressed by stream capture. In fact, beheaded channels (i.e., abandoned downstream reaches) flow through fault-parallel linear valleys and connect to the nearby stream, creating apparent sinistral deflections and perched ponding areas (points s and p, respectively, in fig. 4a). Only the easternmost part of this E-W trending section shows subtle near-fault tectonic landforms, going through the Holocene deposits of the Kaynasli pull-apart basin.

Overall, the 1999 displacement zone closely mimics the long-term tectono-morphologic pattern, since the coseismic vertical component of displacement emphasizes the pre-existing relief [see also Pucci et al., 2006]. Geometry, location and style of the coseismic ruptures, strongly indicate that they have been persistent for a long time (several seismic cycles), along the eastern section of the Düzce Fault (fig. 3b). Moreover, the geomorphic expression of the Düzce Fault testifies that the bulk of the dextral cumulative displacement is localized in a fault zone, that has been experiencing 1999-like surface rupturing for recent, repeated seismic cycles. In particular, the eastern section of the Düzce Fault shows the narrowest and best localized deformation of the fault zone [see Pucci et al., 2007] that allows for a more accurate estimate of its long-term offset and that crosscuts recent continental deposits useful for dating [see Pucci et al., 2008].

3.2. The offset geomorphic markers

Along the western part of the eastern fault section, we recognized offset geomorphic markers, such as river terraces and alluvial fans, related to the drainage network evolution at the outlets to the Düzce Basin. These landforms of the study area are suggested to be climatically-controlled and related to the major alluviation episodes (optima) in the Mediterranean region. In fact, rivers alluviation phases occurred at the end of dry, cooling trends and the rivers degradational phases at the transition from arid to humid conditions [Pucci et al., 2008]. For these river terraces and alluvial fans we reconstructed the original morphology that has been right-laterally dissected by the Düzce Fault motion.

West of Beykoy, we mapped four deflected streams (fig. 4) useful for slip rate calculation assuming a Holocene stream history as follows: (1) the stream was free to flow along a quasi-straight channel and to discharge alluvial deposits with aggradational behavior; (2) because of climatic influence the stream switches to degradational behavior and starts incising within the most recent alluvial surface, the channels remain entrenched and produce terrace remnants [Bull, 1991]; and (3) being unable to change its course, the entrenched stream increases its deflection each time slip occurs on the fault it crosses [Ouchi, 2004, 2005]. At this site, the streams flow north-eastward along entrenched valleys of the range front. When they cross the south-facing fault escarpment, they find as obstacle both bedrock shutter ridges (e.g. spots x, fig. 4a) and remnants of the Holocene alluvial deposits (e.g. spots w, fig. 4a), and turn east to flow along the fault zone (e.g. spots y, fig. 4a). After about a hundred meters, they cut the fault-controlled dam through outlets to the Düzce Basin. The measurement of the deflections of these channels (comparable due to their identical Strahler's [1952] order) yield average cumulative offset of about 106±24 m (fig. 4b). Taking into consideration the assumptions previously explained, in order to establish the timing of the last depositional phase (prior to the stream entrenchment) that likely marks the onset of the stream deflection, we dated the alluvial deposits of the Holocene alluvial remnants. We sampled for radiocarbon dating the top of the remnant of the Holocene alluvial deposits (fig. 4a). The bulk sediment samples provided a calibrated age of of 6720±120 yr BP that represent the onset of the deflection,. This age of the stream deflections translates to a slip rate of 15.7 ± 4 mm/yr for the last ~7000 yrs.

The Develi River is one of the largest water courses of the area (fig. 3). In contrast to the deflected smaller streams, the Develi River is sufficiently large to remove a large volume of sediments as well as any evidence for single coseismic displacement during the interseismic period [e.g. Sugai, 1993]. If this is the case, only features that are not more related to the present dynamics of the streams are suitable evidence for the ongoing deformation (e.g., a flight of abandoned fluvial terraces [Van Dissen and Berryman, 1996]). East of Beykoy, the present-day morphology of the Develi River outlet, shows the presence of remnants of a large Pleistocene alluvial fan, whose sediments have been incised later by the formation of flights of downward-stepping terrace surfaces. At present, the Düzce Fault crosscuts and shifts the alluvial fan deposits far away from the path of the river, sheltering from erosion the north-eastern terraces (II, III, IV). The terrace risers (i.e. erosional scarps between the consecutive terraces) observed on both sides of the Düzce Fault (II-I, III-II, IV-III) offer suitable piercing points for cumulative offset determinations (fig. 5). The radial fan slope is the oldest and highest depositional surface that decreases downfan with a convex-up profile (IV, fig. 5b). The young terrace surfaces are progressively inset and show a downward-stepping flight arrangement shaped by cut-and-fill alluvial behavior (fig. 3b). The displacement of the III–IV and II–III risers and the resultant morphological juxtaposition were not influenced by any other important stream (i.e. capture) or strong erosional process able to substantially modify them. Following this observation, we correlated risers on both sides of the fault and their tectonic evolution was reconstructed. For the III–IV and II–III order risers, we measured 890±110 m and 300±20 m offsets, respectively (fig. 5a). By means of Optically Stimulated Luminescence method, we dated the top of the alluvial deposits of the terraces, which represent the onset of right-lateral tectonic shift at 60,170 ± 6280 yr BP and 21,700 ± 1850 yr BP. These data translate to slip rates of 14±2.1 mm/yr and 15.2±3.5 mm/yr, for the last ~21 ka and ~60 ka, respectively.

Taking into account that ages derive from samples collected in the upper layers of the alluvial surfaces, while the deformations originate from the measurement of younger erosional features, the slip rate calculated by means of such ages should, therefore, be considered a minimum.

Although the calculated slip rates span ages of 7 to 60 ka BP, these values are similar. Assuming a constant slip rate for the past 60 ka, the mathematical linear regressions that interpolate the maximum and the minimum slip rate intervals yield values of 18.2 and 11.8 mm/yr, respectively. These results translate into a mean slip rate of 15.0 mm/yr±3.2 mm/yr (fig. 6).

The north-flowing drainage system of the Düzce area shows further spectacular right-handed deflections of the streams that cross, at high angle, the Düzce Fault. 41 stream deflections, related to cumulative offset of the fault, have been measured (fig. 7a), for the most part of which has not been found any age control to be used for slip-rate estimations. These streams present different Strahler's [1952] order and lithologies of the channel bed, that are supposed to severely influence the stream response to tectonic deflection, mainly by controlling the stream power and the consequent efficiency to remove evidence for coseismic displacements. Figure 7b shows the stream deflection distribution. On the graph are reported curves (cumulative offset curves) obtained by multiplying the 1999 coseismic right-lateral slip distribution curve (fig. 2b) that represent the cumulative offset that is expected, assuming a "characteristic-earthquake model" [Schwartz, and Coppersmith, 1984], due to the repetition of a different number (N) of 1999-like surface rupturing events. Despite the already-mentioned intrinsic differences, apart from few exceptions, the distribution of the stream deflections appear to mimics the curve given by 20-30 1999-like earthquakes. The period of occurrence of the 20-30 1999-like earthquakes, as like as its relative cumulative offset curve, is indicated by the offset of the streams deflected for ca.100 m that was radiocarbon dated about 7000 yr BP (fig. 7b). Summarizing, on the basis of the "characteristic-earthquake model" and constant slip rate assumptions, stream deflections across the Düzce Fault may be explained by repetition of 20-30 1999-like earthquakes during the last 7000 years, thus the recurrence time for surface rupturing events is 290±60 yr. Notably, the deflection of the streams that crosses the Düzce Fault occurred before 7000 BP, at the end of the last deglaciation period (Atlantic, warm and humid climatic conditions [Brocard and Van der Beek, 2006]), indicating the scarce potential of preservation of deflections occurred on previous morphologies that have been re-shaped by last important climatic events.

4. Paleoseismological data

In order to reconstruct the record of last large earthquakes and provide more constraints for the evaluation of earthquake recurrence on the Düzce fault, 10 trenches were excavated at five sites distributed along the entire surface fault trace (for details see Pantosti et al. [2008]). A major goal was the recognition and dating of individual pre-1999 paleoearthquakes and their possible correlation to known historical earthquakes. Consequently, results from previous paleoseismological investigations were compared along with their implications for the seismic behavior of the Düzce segment of the NAFZ.

On the basis of sedimentary and structural relations, evidence for 2 to 3 surface faulting paleoearthquakes predating the 1999 event in all the trenches were found. Because most of the dates recovered from the trenched deposits indicate young ages, thereby preventing the determination of a precise age, radiocarbon dating was integrated with 210Pb analyses and archaeological information (for details see Pantosti et al. [2008]).

Under the assumption that similarly to the 1999 event, paleoearthquakes on the Düzce fault ruptured the whole fault, on the basis of their age compatibility and their local sequence, events between different trenches were correlated (fig. 8). Merging the radiocarbon results obtained from all the trenches, a seismic history for the Düzce fault for the past 1000–1200 years was proposed. Evidence for the Düzce paleoevents was not found in every trench. As a first approach, in absence of clear stratigraphic constraints, the same sequence of events is assumed to be repeated in each trench. Conversely, when no age compatibility exist a different correlation is proposed.

The event DUZ2 occurred between A.D. 1700 and 1900. The 210Pb analysis from Cinarli trench (CIN, fig. 8) and the age estimate of the piece of glass from Aksu trench (fig. 8) suggest that DUZ2 occurred close to A.D. 1900. On the basis of radiocarbon dating, the occurrence of DUZ3 is confined during the past 500 years from trenches CIN, KAY and MEN6 (fig. 8), with the youngest age set to circa A.D. 1700 from 210Pb analysis in CIN trench. Limited evidence and age constraints exist for DUZ4 that falls in the interval A.D. 685–1020. On the basis of stratigraphic considerations from Aksu trench the age of occurrence of DUZ4 can be possibly limited to the range A.D. 890–1020.

There are no obvious correlations of these three surface faulting paleoearthquakes that ruptured the Düzce fault before the November 1999 event with the large events reported in the historical catalogues [Ambraseys and Finkel, 1995; Guidoboni et al., 1994; Guidoboni and Comastri, 2005]. The only historical earthquakes that are known to have produced damage near the Düzce fault are the (1) A.D. 967 that was felt in the area of Bolu, (2) A.D. 1719 earthquake that appears to be a perfect twin of the August 1999 Izmit earthquake, (3) A.D. 1754 that is located in the Sapanca area, (4) A.D. 1878 earthquake that is hypothesized on the Hendek fault or in the Akyazi plain, and (5) A.D. 1894, which occurred on the Izmit fault segment farther west [Ambraseys and Finkel, 1995; Ambraseys, 2002, 2006; Atakan et al., 2002; King et al., 2001] (fig. 8; see fig. 1 for earthquake mezoseismal areas). The A.D. 1719, A.D. 1878, A.D. 1894 and A.D. 967 earthquakes are all compatible with the recognized paleoevents of the Düzce fault. However, given the historical damage reports, only the A.D. 1878 and A.D. 967 earthquakes appear to be good candidates for DUZ2 and DUZ4. Given the low density of population and lack of cultural centers in the area, records of DUZ3 (A.D. 1500–1700) may have been lost or overprinted by the disaster produced by the 1719 earthquake farther west.

Previous paleoseismological investigations [Sugai et al., 2001; Emre et al., 2001, 2003a, 2003b; Hitchcock et al., 2003; Komut, 2005] show evidence for surface faulting paleoearthquakes during the past 2000 years or more. By integrating results from all previous works on the Düzce fault, together with those from Pantosti et al. [2008] the record of last large earthquakes was extended up to the past two millennia, specifically through two older events, at ~A.D. 600 and ~A.D. 200, that were described by Sugai et al. [2001] (fig. 9).

On the basis of the results from this work, four events since A.D. 685–1020 (possibly A.D. 890–1020) yield an average recurrence for the Düzce fault of 380±50 yr (possibly 350±20 yr). If we include paleoearthquakes from previous studies, which reach farther back in time 2000 years, we obtain a similar figure for the average recurrence of 355±35 yr. However, the three most recent events, including 1999, appear more closely spaced. Average recurrence for the four older events (DUZ3 to DUZ6) can range between 460±100 yr, whereas for the three most recent (1999 to DUZ3) can range between 195±55 yr.

4. Comparing geomorphological and paleoseismological results

With the aim of better comprehend the behavioral model of strain accumulation of the Düzce fault, we performed a comparison between slip rates at short and intermediate time scales, from paleoseismological and geomorphological results, respectively, was performed.

Since it was no possible to measure long-term or single paleoevent offsets from trenches, the paleoseismological investigations can only indirectly offer estimimations on the Düzce fault slip rate over the last two millennia. By assuming the Düzce fault as a segment of the NAFZ defined by persistent segment boundaries and by considering the 1999 coseismic slip as representative for the behavior of this fault (assumption of "characteristic earthquake"), we used the seismic record from paleoseismological study coupled with the 1999 surface coseismic slip, to obtain a first approximative picture of fault slip rate. In order to relate the paleoseismological and the geomorphological data, we assigned to each paleoevent 4.0 m of slip per event, that is the average 1999 coseismic horizontal slip (representative of the fault section from which we studied the geomorphic marker offsets) (fig. 2b). In figure 10 we graph the past two millennia paleoevents versus the cumulative slip and we constructed the lines that describe the slip rates in order to compare them with those scaled from the geomorphological analysis. Paleoseismological slip rates are presented as averaged (with related uncertainties) both for all and clusters of the paleoevents.

If we take the most conservative average recurrence time, calculated including all the six events that occurred during the past 2 millennia (i.e., 355±35 yr), the 4.0 m average surface coseismic slip yield a slip rate of 10.2-12.5 mm/a. This short-term slip rate derived from the 1999 maximum slip overlaps with the lower part of that of 11.8–18.2 mm/yr obtained from long-term offset by means of geomorphic markers analysis (fig. 10). The 10 mm/a slip rate derived from GPS measurements [Ayhan et al., 1999, 2001] falls just below the lower value inferred from paleoseismological data. All these data imply that the Düzce fault substantially accommodates, along with the Mudurnu section to the south, the 2 cm/yr of motion along the NAFZ in this area.

Should we consider the paleoseismic record to be complete, the sequence depicted in Figure 9 would be suggestive of earthquake clustering in time. A bimodal paleoearthquakes distribution indicates fluctuations during the past two millennia, with clustered events separated by a longer interseismic interval (967-1719/1754 AD). Since the interseismic interval is not perfectly periodic, the cluster distribution of the paleoearthquakes produces a bimodal slip rate that suggests strain release of the Düzce fault, presenting fluctuations, with clustered high strain release and uniform, low strain release (fig. 10). Over long time intervals, the strain accumulation should be constant and, in the long-term, strain accumulation (from geomorphic markers analysis) and strain release (from paleoseismology) should be the same. In this case, the clustered strain release would recover the small amount of strain energy released before 1700AD, in order to keep constant the short-term slip rate, as exemplified by Wallace-type models (see inset in fig. 10).

5. Discussion and Conclusions

Long-term slip rate estimates of the fault, provided through geomorphological mapping and analysis of fault-related cumulative landforms, were used to calculate recurrence time of the Düzce fault and for a comparison with independent results made available by paleoseismological trenching.

It is critical to determine the timing and distribution of individual faulting events because long-term average slip rates may give grossly incorrect assessments of the hazard potential of a single fault. In addition, evaluation of the characteristics of the entire fault system that contributes to the plate margin deformation, providing a combination of regional and detailed information, is essential for an adequate hazard assessment.

Along the western part of the eastern Düzce fault section, the narrowest and best localized deformation of the fault zone allowed for a more accurate estimate of long-term displacements. Here, offset geomorphic markers, such as river terraces and alluvial fans, were recognized and were used to calculate mean slip rate of 15.0 mm/yr±3.2 mm/yr for the last 60 ka BP. Furthermore, The distribution of spectacular right-handed stream deflections induced by Holocene cumulative offset of the fault, has been estimated to be produced by 20-30 1999-like earthquakes. On the basis of the "characteristic-earthquake model" and constant slip rate assumption, stream deflections across the Düzce Fault may indicate a recurrence time of 290±60 yr for surface rupturing events.

Under the same assumption of "characteristic-earthquake model", the correlation of paleoearthquakes between different trenches along the Düzce fault and the integration of results from previous works show a record of six large earthquakes for the past two millennia. From these paleoearthquakes we obtain an average recurrence time for large earthquakes of 355±35 yr.

The overall average recurrence time for the past two millennia calculated from displaced geomorphic markers and paleoseismological analyses are coherent, presenting ranges of values whose overlap is confined between 320 and 350 years.

Slip rate derived from the average recurrence time of the paleoevents and from the average 1999 coseismic slip of 4.0 m, as slip per event, allows us to estimate, in first approximation, an average slip rate of 11.4 ± 1.1 mm/yr. Comparison between average slip rates from paleoseismological and geomorphological results are comparable, since they present ranges of values overlapping around 12.0 mm/yr.

A detailed analysis of the paleoearthquakes highlights a cluster distribution that produces a bimodal slip rate. This is suggestive of strain release presenting fluctuations in time, with low strain release periods recovered by clustered high strain release periods, indicating a Wallace-type strain release model for the Düzce fault.

Increasing the geological observations is crucial to answer one of the most important questions regarding the significance of the measurements of active surface deformation in the continental lithosphere: what is the relationship between strain accumulation and strain release? On short time scales (years), both strain accumulation and release are monitored using high-precision space-geodetic techniques (GPS; InSAR, etc.). However, on longer time scales (e.g., thousands of years, duration of interseismic intervals), strain accumulation measurements are derived only from geologic strain release data as proxies and more detailed investigations are needed to characterize slip rates and the timing and patterns of faulting events. Near-fault geodetic, paleoseismological, and geological estimates of fault slip rates have been observed to differ (e.g., Basin and Range Province [Friedrich et al. 2003]). In fact, as shown by the Düzce Fault, the average slip rates may remain constant, but variations exist on small time scales larger than the earthquake cycle [Wallace, 1987]. Plate margins, such as the NAFZ along the study area, could present irregularities in crustal thickness, changes in lithology, local variations of the regional stress systems and complex structural style of the active fault system originated from the tectonic inheritance. In these regions, non-uniformity of occurrence of large slip events on seismogenic faults and small time scale variations of slip rates probably are normal characteristic of faulting.

Captions

FIG.1 Simplified trace of the North Anatolian Fault Zone west of the Bolu basin (see lower right inset for location of the area). Portions of the fault zone that ruptured during the 1999 earthquakes are shown. The mezoseismal areas of the historical earthquakes occurred near the Düzce fault segment are shown too [from Ambraseys and Ambraseys, 2002; Atakan, 2002; King et al., 2001].

FIG.2 a) Trace of the 1999 surface ruptures along the Düzce fault (see dashed rectangle in fig.1 for location) and location of the five trench sites (rectangles; KAY: Kaynasli; MEN: Mengencik; CH: Cakir Haci Ibrahim; CIN: Cinarli; AK: Aksu). Numbered hexagons are locations where trenching from other authors was performed (1. Hitchcock et al., 2003; 2. Komut, 2005; 3. Emre et al. 2001, 2003a and 2003b; 4. Sugai et al., 2001). Dashed rectangles indicate the location of geomorphic marker analysis. b) Horizontal slip distribution along the 1999 surface ruptures in the study area.

FIG.3 Simplified geomorphological and coseismic fault scarp map of the two parts of the Düzce Fault. a) Western section. b) Eastern section. Continental deposits from 1:20.000 scale field survey, bedrock from Herece and Akay [2003]. Letters indicate locations discussed in the text. Contour interval 100 m. (see fig. 2a for location).

FIG.4 a) Simplified geomorphological map of a streams offset area. Contour interval 10 m. (see fig. 3b for location). b) Stream deflection measurements. Dashed lines indicate the possible projections on the fault of the stream channels. Dotted white lines indicate the piercing points used for offset calculations. 1:18.000 scale aerial-photo on the background.

FIG.5 a) Terrace risers (IV-III and III-II) are severely offset. Dashed lines indicate the possible projections on the fault of the terrace risers. Dotted lines indicate the piercing points used for offset calculations. 1:18.000 scale aerial-photo on the background. b) Oblique view of the pressure ridge and the terrace risers (see fig. a for view direction). Labels III and IV refer to terrace order. Small red arrows point to the coseismic rupture trace. Hexagons locates sampling sites for OSL dating. (see fig.3b for location).

FIG.6 Slip rate diagram of the Düzce Fault. The slip rates calculated at different time-scales and for different geomorphic markers (fig.4 and fig.5) are reported along with the interpolated uniform slip rate.

FIG.7 Stream deflection distribution. Bars indicate the stream location and amount of the offset, thin bars indicate uncertainties. black curves indicate cumulative offset curve obtained by multiplying the 1999 coseismic right-lateral slip distribution (fig. 2b). Thick gray curve is the envelope of the maximum stream offsets.

FIG.8 Correlation of paleoearthquakes and inferred age ranges. The upper panel shows the radiocarbon age probability distribution, as well as the

210Pb and the archaeological estimates used to set the age of an event horizon in each trench. Black arrows indicate whether the sample pre-dates or postdates the event. Dashed gray lines indicate a preferred age for the event. The middle panel shows the correlations among trenches. Gray horizontal lines represent the best age range for the event. Dark gray rectangles show preferred ages of events. Correlated events (DUZ2 to DUZ4) represent pre-1999 surface faulting earthquakes that ruptured the same fault extent as in 1999. In the lower panel historical earthquakes (stars) known to have occurred in proximity of the Düzce fault are reported.

FIG.9 Integration of paleoseismological results from this work and previous ones. Ellipses show the age range uncertainties for paleoearthquakes. Correlated historical earthquakes are shown too (stars). Recent earthquakes appear to have occurred more closely spaced than previous ones.

FIG.10 Comparison between slip rates from paleoseismological and geomorphological results. Shaded areas show average slip rate uncertainties for both dataset. Light gray ellipses and stars show the seismic record of the last two millennia. 1999-like slip per event is assigned. Dashed lines indicate the short-term slip rate fluctuations suggested by the paleoevents. The inset shows the Wallace-type strain release model [1987] (modified from Friedrich et al. [2003]).

References

Akyüz, H.S., A.A. Barka, E. Altunel, R.D. Hartleb, and G. Sunal (2000), Field observations and slip distribution of the November 12, 1999 Düzce earthquake (M=7.1), Bolu - Turkey. In: A.A. Barka et al. (Eds.), The 1999 Izmit and Düzce earthquakes; preliminary results. Istanbul Technical University, Istanbul, Turkey, pp. 63-70.

Akyüz, H.S., R.D. Hartleb, A.A. Barka, E. Altunel, G. Sunal, B. Meyer and R. Armijo (2002), Surface rupture and slip distribution of the 12 November 1999 Düzce earthquake (M7.1), North Anatolian Fault, Bolu, Turkey, *Seism. Soc. Am. Bull.*, 92 (1), 61-66.

Ambraseys, N.N, (2002), The seismic activity of the Marmara Sea region over the last 2000 years, *Seism. Soc. Am. Bull.*, 92 (1), 1-18.

Ambraseys, N. N. (2006), Comparison of frequency of occurrence of earthquakes with slip rates from long-term seismicity data: The cases of Gulf of Corinth, Sea of Marmara and Dead Sea Fault Zone, *Geophys. J. Int.*, 165, 516– 526.

Ambraseys N.N. and C.F. Finkel (1995). The seismicity of Turkey and adjacent areas: a historical review, 1500-1800, Muhittin Salih Eren, 240 pp., Istanbul.

Armijo, R., B. Meyer, A. Hubert and A.A. Barka (1999), Westward propagation of the North Anatolian fault into the northern Aegean: Timing and kinematics, *Geology*, 27 (3), 267-270.

Ayhan, M.A., C. Demir, A. Kilicoglu, I. Sanli, and S.M. Nakiboglu (1999), Crustal motion around the western segment of the north Anatolian fault zone: geodetic measurements and geophysical interpretation. International Union of Geodesy and Geo-physics (IUGG99), Birmingham, United Kingdom, 18-30 July.

Ayhan, M.E., R.B¨urgmann, S. McClusky, O. Lenk, B. Aktug, E. Herece and R.E. Reilinger, 2001. Kinematics of the Mw = 7.2, 12 November 1999, Düzce, Turkey earthquake, *Geophys. Res. Lett.*, 28 (2), 367-370.

Atakan, K., A. Ojeda, M. Meghraoui, A.A. Barka, M. Erdik and A. Bodare (2002), Seismic hazard in Istanbul following the 17 August 1999 Izmit and 12 November 1999 Duzce earthquakes, *Seism. Soc. Am. Bull.*, 92 (1), 466-482.

Barka, A.A., 1992. The North Anatolian fault zone. *Ann. Tecton.* 6, 164–195.

Brocard, G.Y, and P.A. Van der Beek (2006), Influence of incision rate, rock strength, and bedload supply on bedrock river gradients and valley-flat widths; field-based evidence and calibrations from western Alpine rivers (southeast France), Special Paper - *Geological Society of America*, 398, 101-126.

Bull,W.B., 1991. Geomorphic Responses to Climatic Change. Oxford University Press, London, UK, p. 326.

Canıtez, N. and B. Üçer (1967), Computer determinations for the fault plane solutions in and near Anatolia, *Tectonophysics*, 4, 235-244.

Christie-Blick, N. and K.T. Biddle (1985), Deformation and basin formation along strike-slip faults, in: Strike-slip Deformation, Basin Formation and Sedimentation, K.T. Biddle and N. Christie-Blick (Editors), *Soc.Econ. Paleont. Min. Spec. Publ.*, 1-34.

Dewey, J.F., M.R. Hempton, W.S.F. Kidd, F. Saroglu and A.M.C. Şengör (1986), Shortening of continental lithosphere; the neotectonics of eastern Anatolia, a young collision zone, *Geological Society Spec. Pub.*, 19, 3-36.

Emre, Ö., T.Y. Duman, S. Toda, M. Okuno, A. Dogan, S. Ozalp, H. Tsutsumi, F. Tokay, T. Haraguchi, H. Kondo, N. Subito and T. Nakamura (2001), Paleoseismologic Findings on the Düzce Fault: North Anatolian Fault Zone, NW Turkey, American Geophysical Union, Fall Meeting 2001, abstract.

Emre, Ö., Y. Awata and T. Duman (Eds.) (2003a), Surface rupture associated with the 17 August 1999 Izmit earthquake. General Directorate of Mineral Research and Exploration, Ankara, Turkey, ISBN: 975-6595-53-1, pp. 29–271.

Emre, Ö., S. Toda, T.Y. Duman, T. Sugai, A. Dogan, Y. Awata, M.Okuno, H. Tsutsumi, S. Ozalp and F. Tokay (2003b), Recurrence of the large earthquakes on the 1999 Izmit and Düzce surface ruptures, North Anatolian Fault, Turkey. EGS-AGU-EUG Joint Assembly, Abstracts, 6-11 April 2003, Nice, France.

Friedrich, A.M., B.P. Wernicke, N.A. Niemi, R.A. Bennett and J.L. Davis (2003), Comparison of geodetic and geologic data from the Wasatch region, Utah, and implications for the spectral character of Earth deformation at periods of 10 to 10 million years, *J. of Geophys. Res.*, vol. 108, B4, 2199, doi:10.1029/2001jb000682,

Guidoboni, E., and A. Comastri (2005), Catalogue of Earthquakes and Tsunamis in the Mediterranean Area From the 11th to the 15th Century, 1037 pp., Storia Geofis. Ambiente, Bologna, Italy.

Guidoboni, E., A. Comastri, and G. Traina (1994), Catalogue of Ancient Earthquakes in the Mediterranean Area Up to the 10th Century, 504 pp., Storia Geofisica Ambiente, Bologna, Italy.

Herece, E., and E. Akay (2003), 1:100.000 geological maps of the North Anatolian Fault, General Directorate of Mineral Research and Exploration, Ankara, Appendix 3 and 4.

Hitchcock, C., E. Altunel, A.A Barka, J. Bachhber, W. Lettis, Ö. Kozci, J. Helms and S. Lindvall (2003), Timing of Late Holocene earthquakes on the eastern Düzce fault and implications for slip transfer between the southern and the northern strands of the North Anatolian Fault System, Bolu, Turkey, *Turkish J. Earth Sci.*, 12 (1), 119-136.

Jackson, J. and D. McKenzie (1988). The relationship between plate motions and seismic moment tensors, and the rates of active deformation in the Mediterranean and Middle East, *Geoph. J. Int.*, 93 (1), 45-73.

Johnson, A. M., R. W. Fleming, and K. M. Cruikshank (1994), Shear zones formed along long, straight traces of fault zones during the 28 June 1992 Landers, California, earthquake, *Bull. Seism. Soc. Am*, **84,** 499–510.

Kahle H. G., M. Cocard, Y. Peter, A. Geiger, R. Reilinger, S.C. McClusky, R. King, A. Barka and G. Veis (1999), GPS-derived strain rate field within the boundary zones of the Eurasian, African, and Arabian Plates, *J. Geophy. Res.* 105 (B3), 23 353-23 370.

Kahle H. G., M. Cocard, Y. Peter, A. Geiger, R. Reilinger, A. Barka and G. Veis (2000), GPS-derived strain rate field within the boundary zones of the Eurasian, African, and Arabian Plates, *J. Geophy. Res.*, 105 (B3), 23 353-23 370.

King, G.C.P., A. Hubert-Ferrari, S.S. Nalbant, B. Meyer, R. Armijo and D.D. Bowman (2001), Coulomb interactions and the 17 August 1999 Izmit, Turkey earthquake, Comptes Rendus de l'Academie des Sciences, Serie II. Sciences de la Terre et des Planetes, 333 (9), 557-569.

Komut T., (2005), Paleoseismological studies on Düzce fault and geological data on the seismogenic sources in the vicinity of Düzce area, Kandilli Observatory and Earthquake Research Institute Boğaziçi University, Ph.D. Thesis, pp. 155.

Lazarte, C.A., J.D. Bray, A.M. Johnson, and R.E. Lemmer (1994), Surface breakage of the 1992 Landers earthquake and its effects on structures, *Bull. Seism. Soc. Am*, 84**,** 547–561.

McClusky, S.C., A. Balassanian, A.A. Barka, C. Demir and S. Ergintav (2000). Global positioning system constrain on plate kinematics and dynamics in the eastern Medditerranean and Caucasus, *J. Geophy. Res.*, 105 (B3), 5695-5720.

McKenzie, D.P., (1972), Active tectonics of the Mediterranean region, Geophys. J. R. Astron. Soc., 30, 109-185.

Okay, A.I., E. Demirbag, H.N. Kurt, and I. Kuşçu (1999), An active, deep marine strike-slip basin along the North Anatolian Fault in Turkey, *Tectonics*, 18 (1), 129-147.

Ouchi, S., 2004. Flume experiments on the horizontal stream offset by a strike-slip fault. *Earth Surf. Processes Landf.* 29, 161–173.

Ouchi, S., 2005. Development of offset channels across the San Andreas fault. *Geomorphology* 70, 112–128.

Pantosti, D., S. Pucci, P.M. De Martini, N. Palyvos, G. D'Addezio and C. Zabci (2008), Paleoseismological investigation along the Duzce segment of the North Anatolian Fault Zone (Ms 7.1, Nov. 1999), *Journal of Geophysical Research-Solid Earth*, 113, B01309, doi:10.1029/2006JB004679.

Parsons, T., S. Toda, R.S. Stein, A. Barka and J.H. Dieterich (2000), Heightened odds of large earthquakes near Istanbul: an interaction-based probability calculation, *Science*, 288, 661–664.

Pucci, S., N. Palyvos, C. Zabci, D. Pantosti (2006): Coseismic ruptures and associated tectonic landforms along the Duzce segment of the North Anatolian Fault Zone (Ms 7.1, Nov. 1999), *Journal of Geophysical Research-Solid Earth*, 111, B06312, doi:10.1029/2004JB003578.

Pucci, S., D. Pantosti, M. Barchi and N. Palyvos (2007), A Complex seismogenic shear zone: the Düzce segment of the North Anatolian Fault Zone (Turkey), *Earth Planetary Science Letters*, 262, 185–203, doi:10.1016/j.epsl.2007.07.038.

Pucci, S., P.M. De Martini and D. Pantosti (2008): Preliminary slip rates of the Duzce segment of the North Anatolian Fault Zone from offsets geomorphic markers, *Geomorphology*, 97, 538–554.

Reilinger, R.E., S.C. McClusky, M.B. Oral, W. King and M.N. Toksöz (1997), Global Positioning, System measurements of present-day crustal movements in the Arabian-Africa-Eurasia plate collision zone. *J. Geophy. Res.* 102 (B5), 9983-9999.

Reinecker, J., O. Heidbach, M. Tingay, P. Connolly, and B. Müller (2004), The 2004 release of the World Stress Map (available online at www.world-stress-map.org).

Şaroğlu, F., Ö. Emre and İ. Kuşçu (1992). Active fault map of Turkey. General Directorate of Mineral Research and Exploration, Ankara.

Schwartz, D.P., and K.J. Coppersmith (1984), Fault behavior and characteristic earthquakes; examples from the Wasatch and San Andreas fault zones, *J. Geophys. Res.*, 89 (7B), 5681-5698.

Şengör, A.M.C., (1979), The North Anatolian transform fault: Its age, offset and tectonic significance, *J. Geol. Soc. London*, 136, 269-282.

Şengör, A.M.C., N. Görür and F. Şaroğlu (1985), Strike-slip faulting and related basin formation in zones of tectonic escape; Turkey as a case study, In Biddle, K.T., and N. Christie-Blick (Eds.) Strike-slip Deformation, Basin Formation and Sedimentation, *Soc. Econ. Paleont. Min. Spec. Publ.*, 37, 227-264.

Şengör, A.M.C., O. Tüysüz, C. İmren, M. Sakınç, H. Eyidoğan, N. Görür, X. Le Pichon and C. Rangin (2005), The North Anatolian Fault: a new look, *Annu. Rev. Earth Planet. Sci.*, 33, 37-112.

Sieh, K.L., L. Jones, E. Hauksson, K. Hudnut, D. Eberhart-Phillips, T.H. Heaton, S. Hough, K. Hutton, H. Kanamori, A. Lilje, S. Lindvall, S.F. McGill, J. Mori, C. Rubin, J.A. Spotila, J. Stock, H.K. Thio, J. Treiman, B. Wernicke, and J. Zachariasen (1993), Near-field investigations of the Landers earthquake sequence, April to July, 1992, *Science*, 260**,** 171–176.

Strahler, A.N., (1952), Dynamic basis of geomorphology, *Geol. Soc. Am. Bull.*, 63, 923-938.

Straub, C., H. G. Kahle, and C. Schindler (1997), GPS and geologic estimates of the tectonic activity in the Marmara Sea region, NW Anatolia, *J. Geophys. Res.*, 102 (B12), 27 587-27 601

Sugai, T., 1993. River terrace development by concurrent fluvial processes and climate change. *Geomorphology* 6, 243–252.

Sugai, T., Y. Awata, S. Toda, Ö. Emre, A. Dogan, S. Ozalp, T. Haraguchi, H. Kinoshita, K. Takada, and M. Yamaguchi (2001), Paleoseismic investigation of the 1999 Du¨zce earthquake fault at Lake Efteni, North Anatolian fault system, Turkey, Annu. Rep. Active Fault Paleoearthquake Res. 1, Active Fault Res. Cent., Tsukuba, Japan.

Tchalenko, J.S. and N.N. Ambraseys (1970), Structural analysis of the Dasht-e Bayaz (Iran) earthquake fractures, *Geol. Soc. Am. Bull.*, 81, 1, 41-59.

Tchalenko, J.S., and M. Berberian (1975), Dasht-e Bayaz fault, Iran: earthquake and earler related structures in bedrock, *Geol. Soc. Am. Bull.*, 86, 703–709.

Van Dissen, R., and K.R. Berryman (1996), Surface rupture earthquakes over the last ~1000 years in the Wellington region, New Zealand, and implications for ground shaking hazard, *J. Geophys. Res.*, 101, B3, 5999-6019.

Wallace, R. E. (1987), Grouping and migration of surface faulting and variation in slip rates on faults in the Great Basin province, *Bull. Seismol. Soc. Am.*, 77, 868–877.

Westaway, R., (1994), Present-day kinematics of the Middle-East and Eastern Mediterranean, *J. Geophys. Res*, 99, 12 071-12 090.

Wong, H K, T. Luedmann, A. Ulug and N. Gorur (1995), The Sea of Marmara; a plate boundary sea in an escape tectonic regime, *Tectonophysics*, 244 (4), 231-250.

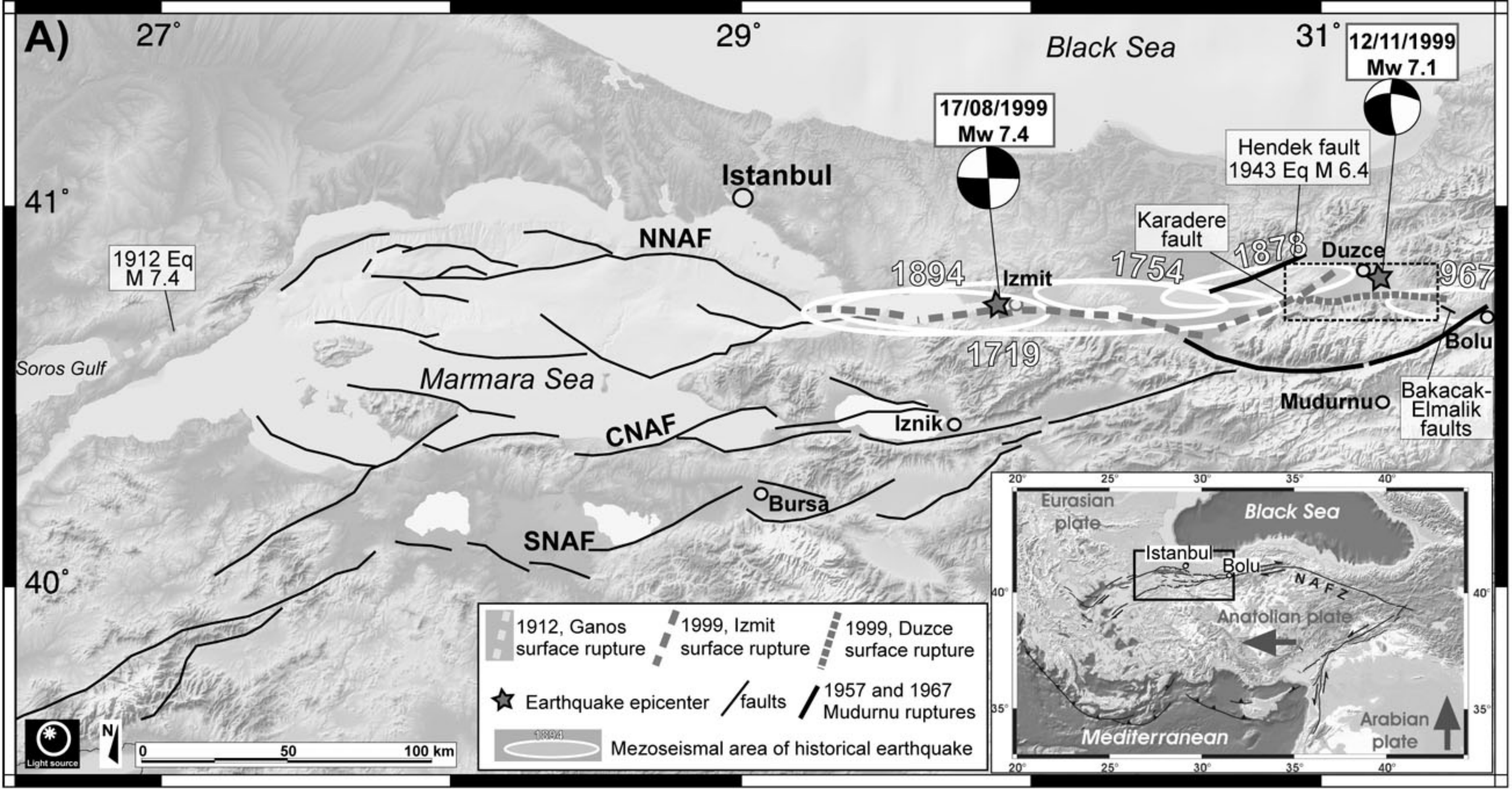

A)
27°
29°
31°
41°
40°
Black Sea
12/11/1999
Mw 7.1
17/08/1999
Mw 7.4
Hendek fault
1943 Eq M 6.4
Istanbul
Karadere
fault
NNAF
1878
Duzce
1754
1894
Izmit
967
1912 Eq
M 7.4
1719
Bolu
Soros Gulf
Marmara Sea
Bakacak-
Elmalik
faults
Mudurnu
Iznik
CNAF
Bursa
SNAF
1912, Ganos
surface rupture
1999, Izmit
surface rupture
1999, Duzce
surface rupture
Earthquake epicenter
faults
1957 and 1967
Mudurnu ruptures
Mezoseismal area of historical earthquake
Light source
N
0
50
100 km
Eurasian
plate
Black Sea
Istanbul
Bolu
NAFZ
Anatolian plate
Mediterranean
Arabian
plate
20°
25°
30°
35°
40°

Fig. 1

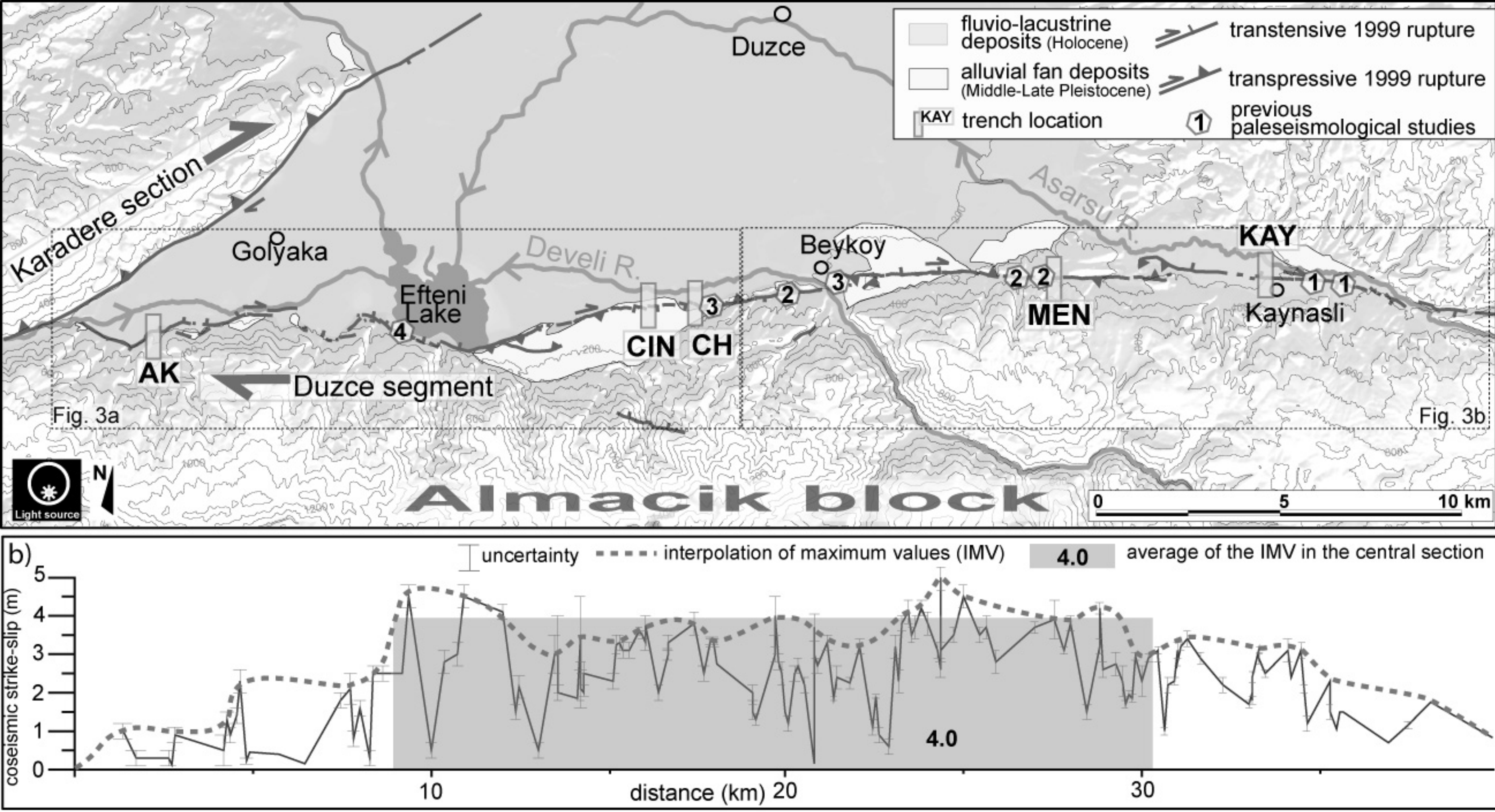

fluvio-lacustrine deposits (Holocene)
alluvial fan deposits (Middle-Late Pleistocene)
KAY trench location
transtensive 1999 rupture
transpressive 1999 rupture
previous paleseismological studies
Duzce
Karadere section
Golyaka
Efteni Lake
Develi R.
Asarsu R.
Beykoy
Kaynasli
AK
CIN
CH
MEN
KAY
Duzce segment
Fig. 3a
Fig. 3b
Almacik block
Light source
N
0
5
10 km
b)
uncertainty
interpolation of maximum values (IMV)
4.0
average of the IMV in the central section
coseismic strike-slip (m)
distance (km)

Fig. 2

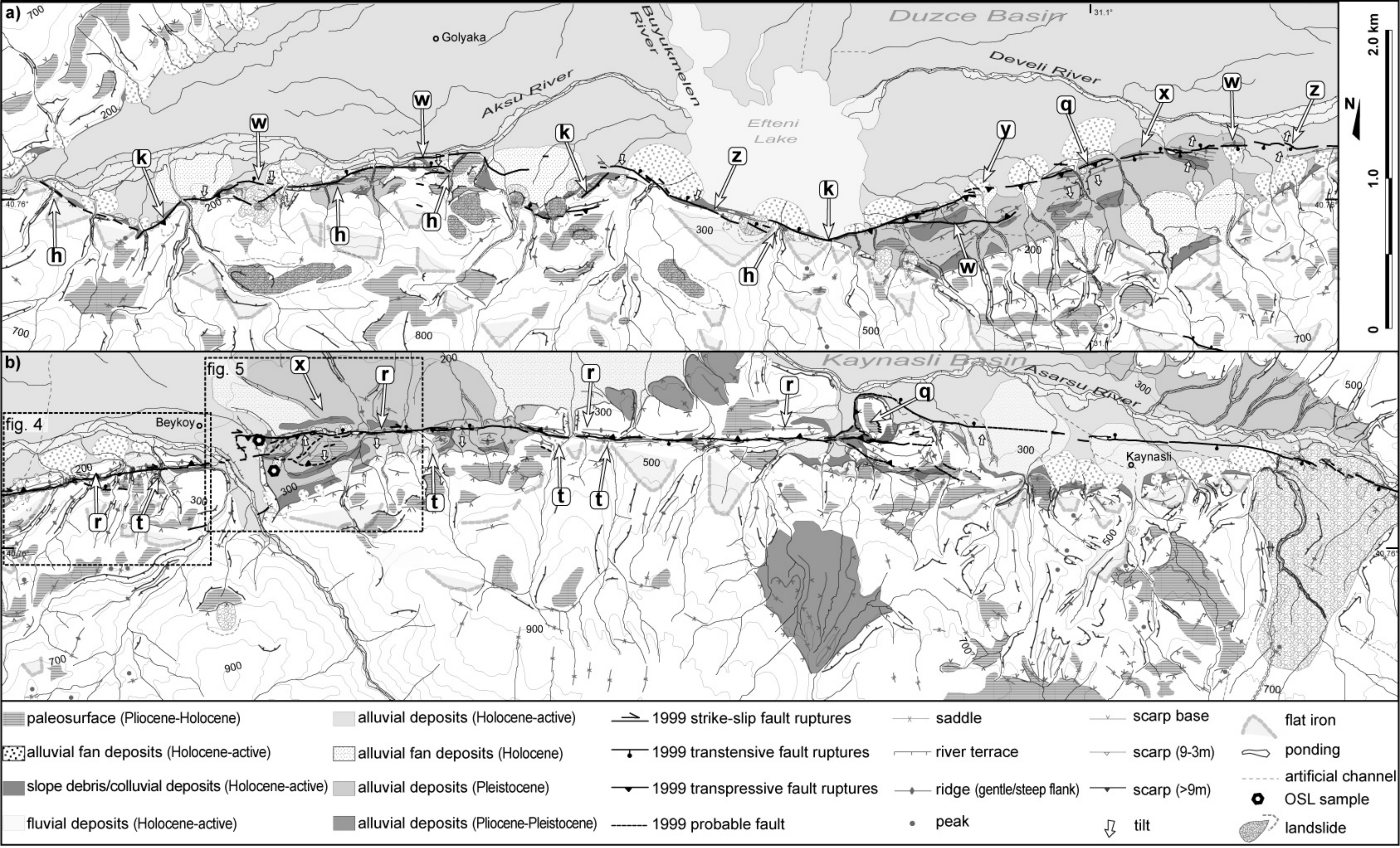
a)
Duzce Basin
Golyaka
Buyukmelen River
Aksu River
Develi River
Efteni Lake
2.0 km
1.0
0
N
b)
Kaynasli Basin
Asarsu River
Beykoy
Kaynasli
fig. 4
fig. 5
paleosurface (Pliocene-Holocene)
alluvial fan deposits (Holocene-active)
slope debris/colluvial deposits (Holocene-active)
fluvial deposits (Holocene-active)
alluvial deposits (Holocene-active)
alluvial fan deposits (Holocene)
alluvial deposits (Pleistocene)
alluvial deposits (Pliocene-Pleistocene)
1999 strike-slip fault ruptures
1999 transtensive fault ruptures
1999 transpressive fault ruptures
1999 probable fault
saddle
river terrace
ridge (gentle/steep flank)
peak
scarp base
scarp (9-3m)
scarp (>9m)
tilt
flat iron
ponding
artificial channel
OSL sample
landslide

Fig. 3

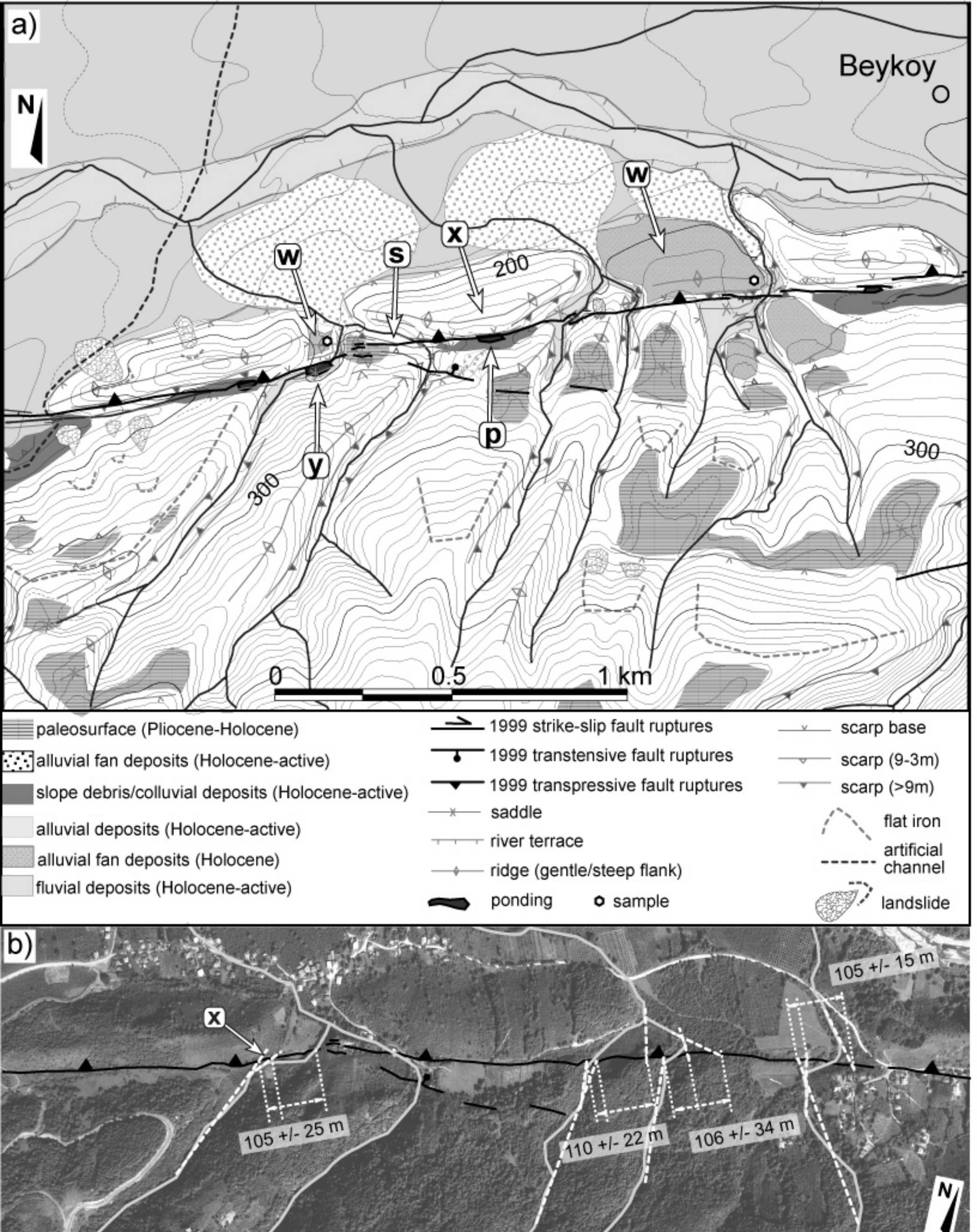
a)
Beykoy
N
w
s
x
w
200
y
p
300
300
0
0.5
1 km
paleosurface (Pliocene-Holocene)
alluvial fan deposits (Holocene-active)
slope debris/colluvial deposits (Holocene-active)
alluvial deposits (Holocene-active)
alluvial fan deposits (Holocene)
fluvial deposits (Holocene-active)
1999 strike-slip fault ruptures
1999 transtensive fault ruptures
1999 transpressive fault ruptures
saddle
river terrace
ridge (gentle/steep flank)
ponding
sample
scarp base
scarp (9-3m)
scarp (>9m)
flat iron
artificial channel
landslide
b)
x
105 +/- 15 m
105 +/- 25 m
110 +/- 22 m
106 +/- 34 m
N

Fig. 4

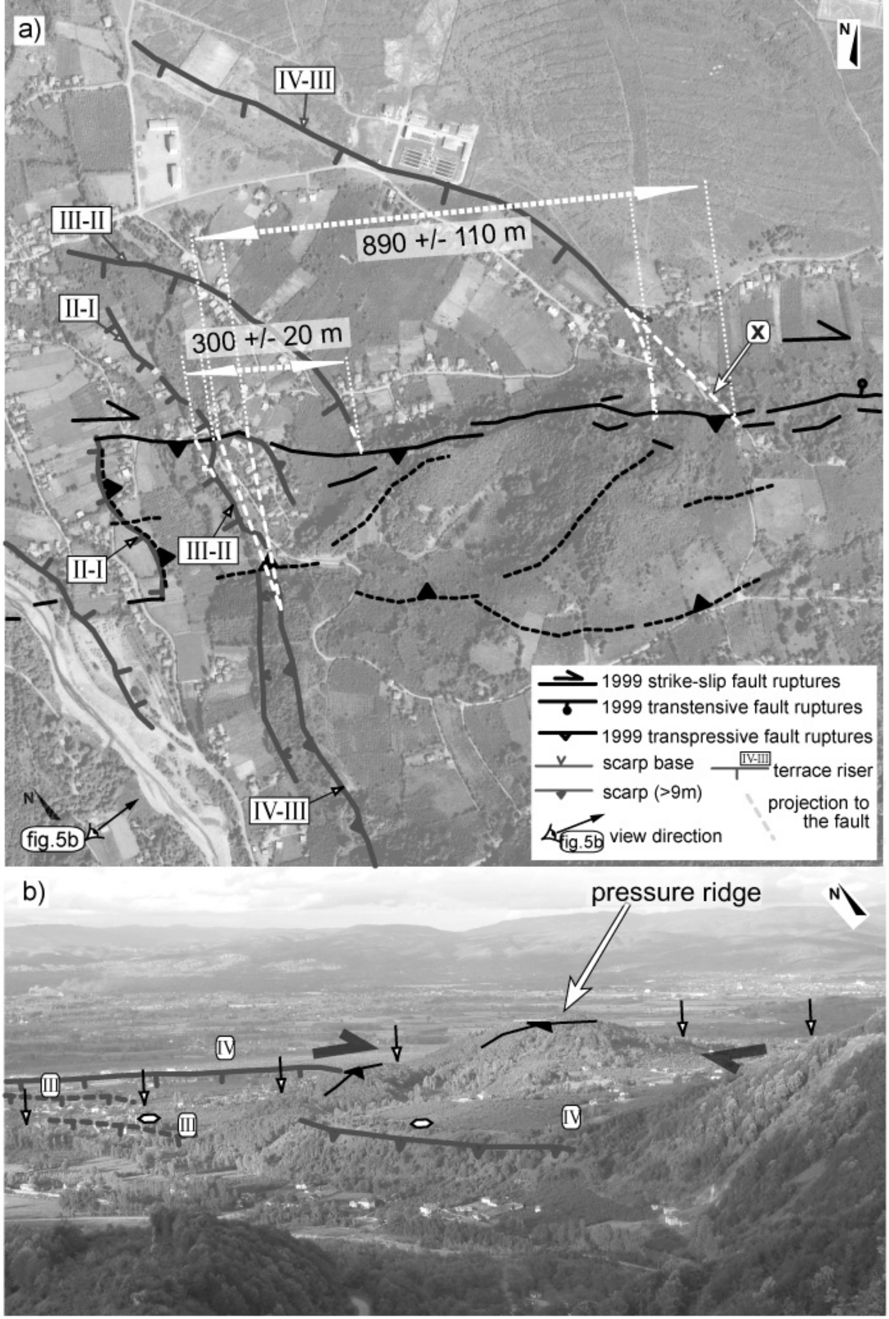
a)
N
IV-III
III-II
890 +/- 110 m
II-I
300 +/- 20 m
X
III-II
II-I
IV-III
N
fig.5b
1999 strike-slip fault ruptures
1999 transtensive fault ruptures
1999 transpressive fault ruptures
scarp base
IV-III
terrace riser
scarp (>9m)
projection to the fault
fig.5b
view direction
b)
pressure ridge
N
IV
III
III
IV

Fig. 5

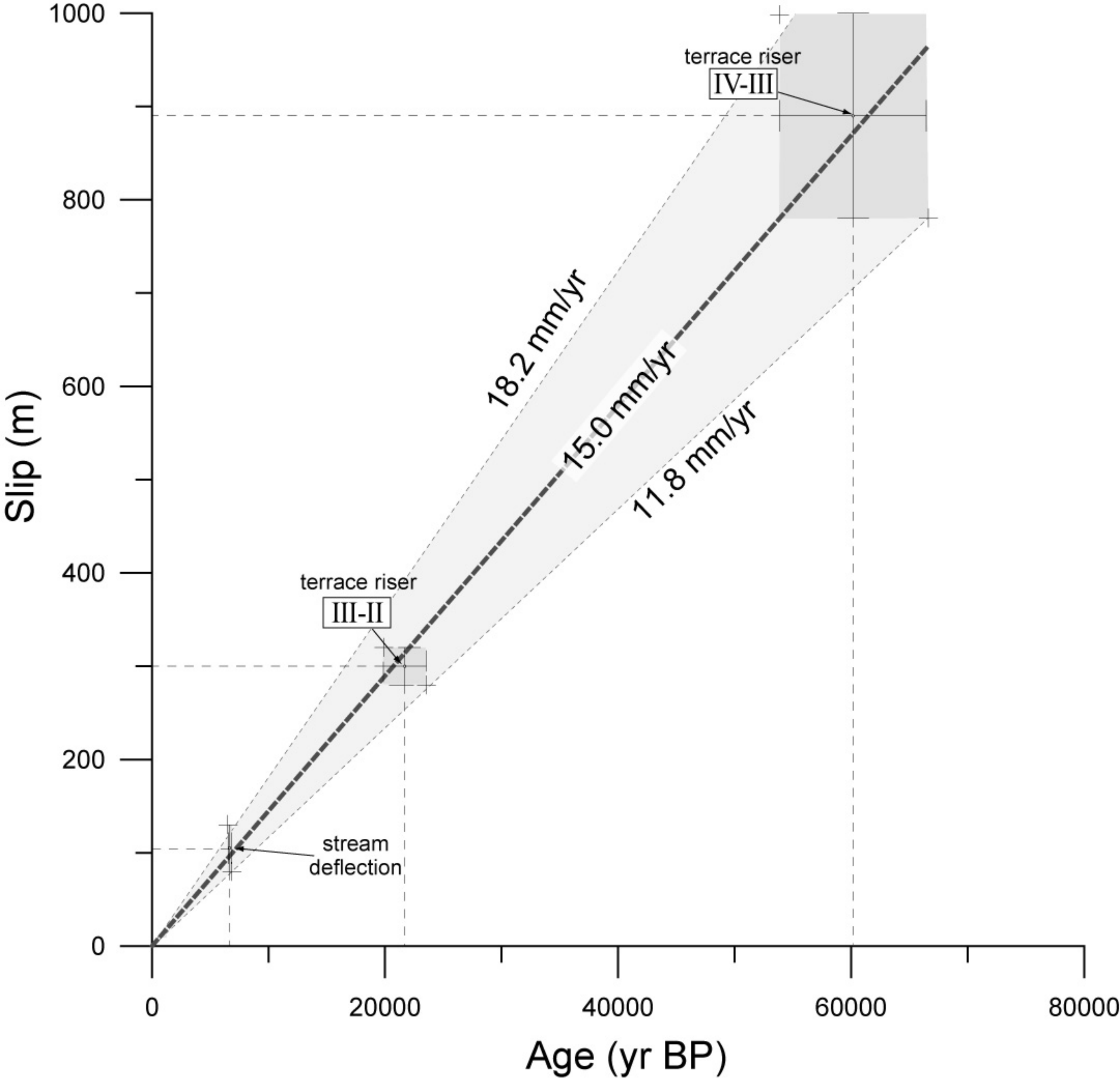
terrace riser
IV-III
terrace riser
III-II
stream
deflection
18.2 mm/yr
15.0 mm/yr
11.8 mm/yr
Slip (m)
Age (yr BP)
0
200
400
600
800
1000
0
20000
40000
60000
80000

Fig. 6

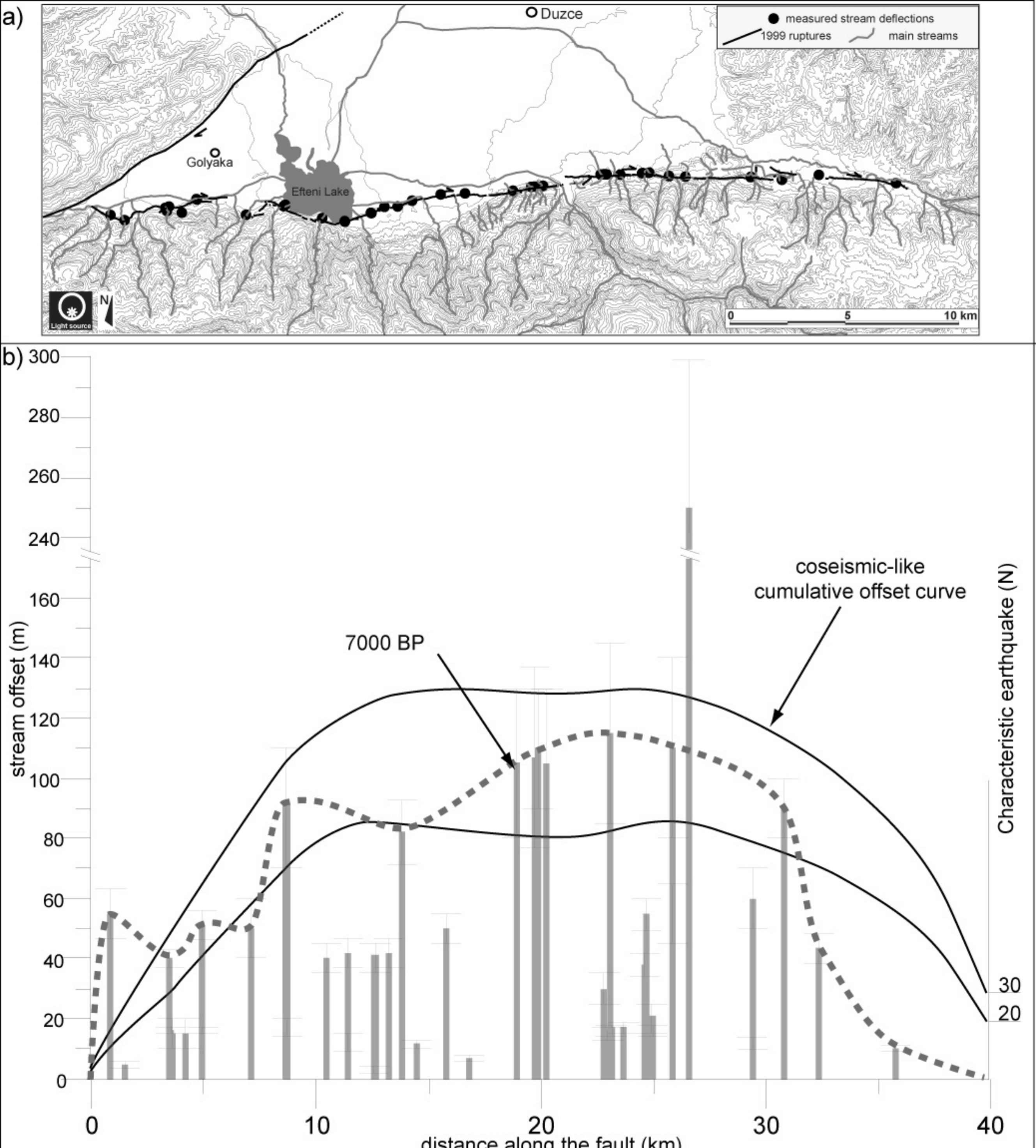
a)
Duzce
measured stream deflections
1999 ruptures
main streams
Golyaka
Efteni Lake
Light source
N
0
5
10 km
b)
stream offset (m)
distance along the fault (km)
coseismic-like
cumulative offset curve
7000 BP
Characteristic earthquake (N)
30
20
0
10
20
30
40
300
280
260
240
160
140
120
100
80
60
40
20
0

Fig. 7

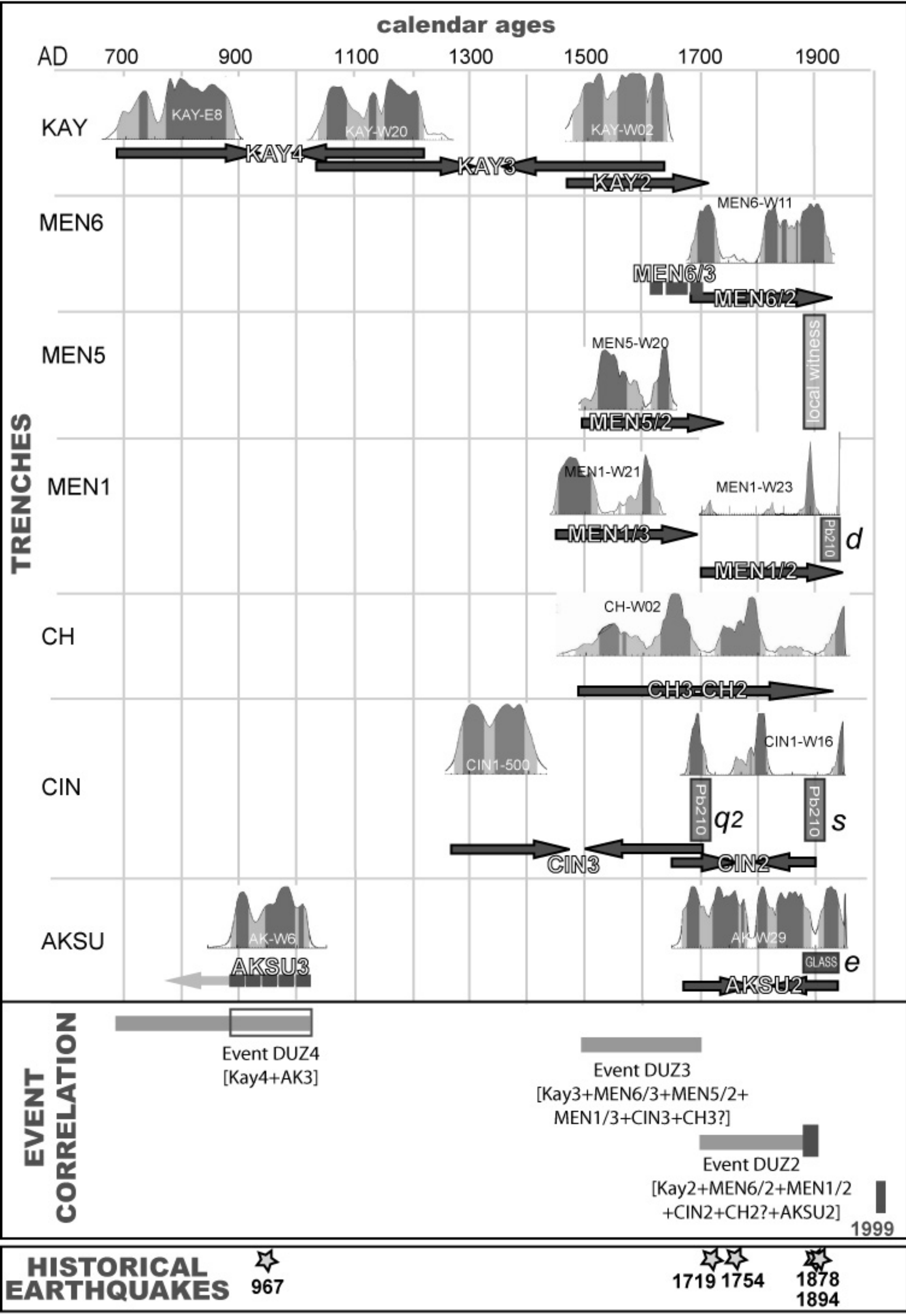
calendar ages
AD 700 900 1100 1300 1500 1700 1900
TRENCHES
KAY
KAY-E8
KAY-W20
KAY-W02
KAY4
KAY3
KAY2
MEN6
MEN6-W11
MEN6/3
MEN6/2
MEN5
MEN5-W20
MEN5/2
local witness
MEN1
MEN1-W21
MEN1-W23
MEN1/3
Pb210
d
MEN1/2
CH
CH-W02
CH3-CH2
CIN
CIN1-500
CIN1-W16
Pb210
q2
Pb210
s
CIN3
CIN2
AKSU
AK-W6
AK-W29
GLASS
e
AKSU3
AKSU2
EVENT CORRELATION
Event DUZ4
[Kay4+AK3]
Event DUZ3
[Kay3+MEN6/3+MEN5/2+
MEN1/3+CIN3+CH3?]
Event DUZ2
[Kay2+MEN6/2+MEN1/2
+CIN2+CH2?+AKSU2]
1999
HISTORICAL EARTHQUAKES
967
1719
1754
1878
1894

Fig. 8

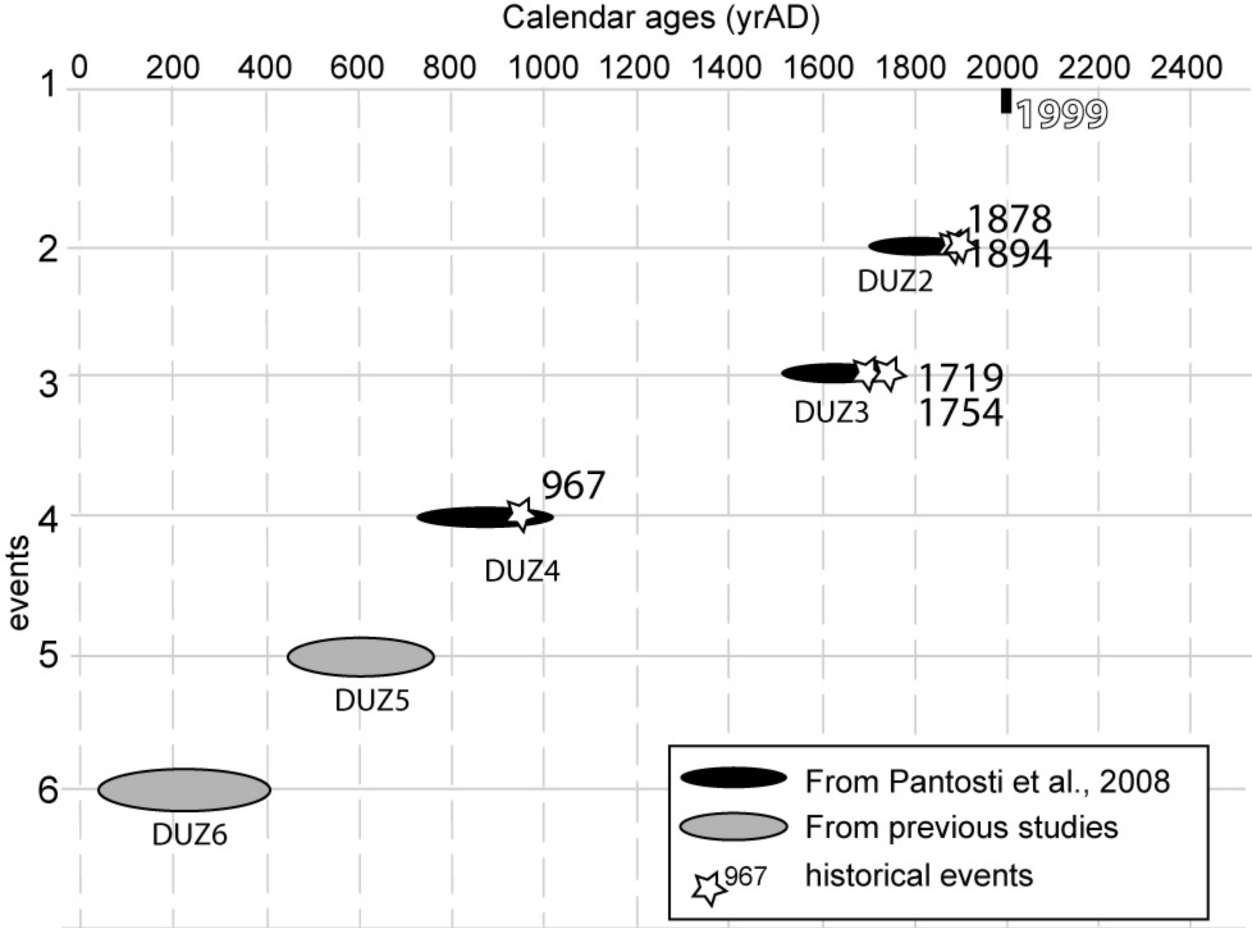
Calendar ages (yrAD)
0
200
400
600
800
1000
1200
1400
1600
1800
2000
2200
2400
1
2
3
4
5
6
events
1999
1878
1894
DUZ2
1719
1754
DUZ3
967
DUZ4
DUZ5
DUZ6
From Pantosti et al., 2008
From previous studies
967
historical events

Fig. 9

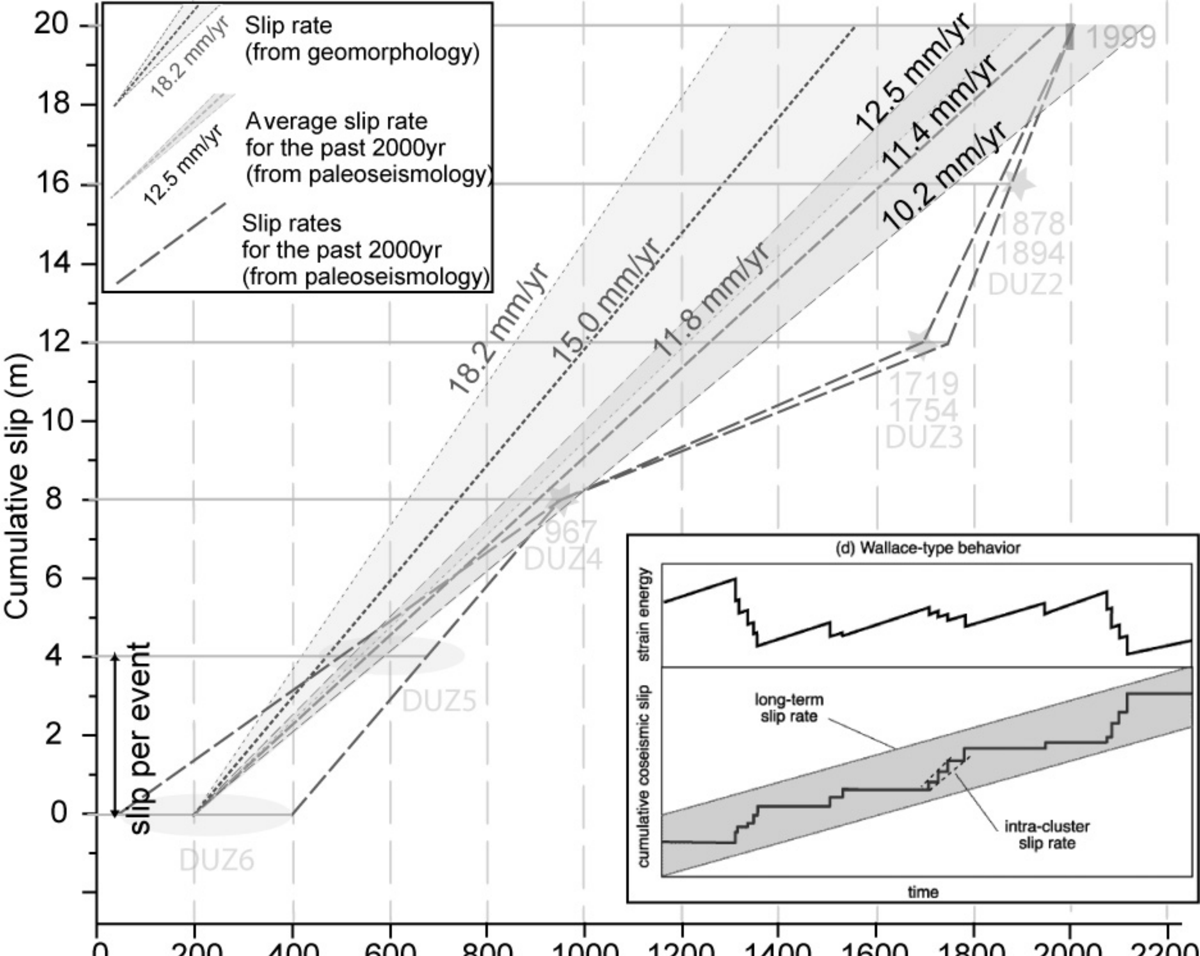

Slip rate
(from geomorphology)
18.2 mm/yr
Average slip rate
for the past 2000yr
(from paleoseismology)
12.5 mm/yr
Slip rates
for the past 2000yr
(from paleoseismology)
18.2 mm/yr
15.0 mm/yr
11.8 mm/yr
12.5 mm/yr
11.4 mm/yr
10.2 mm/yr
1999
1878
1894
DUZ2
1719
1754
DUZ3
967
DUZ4
DUZ5
DUZ6
slip per event
Cumulative slip (m)
Calendar ages (yrAD)
0
200
400
600
800
1000
1200
1400
1600
1800
2000
2200
2
4
6
8
10
12
14
16
18
20
(d) Wallace-type behavior
strain energy
cumulative coseismic slip
long-term
slip rate
intra-cluster
slip rate
time

Fig. 10